Article ID: 1000-7032(2018)04-0457-09

Synthesis and Luminescence Properties of Red Phosphor $BaZn_2(BO_3)_2:Eu^{3+}$ for Light-emitting Diode

WU Cheng-xiao[1], DENG De-gang[1*], RUAN Feng-ping[1], YU Hua[2], XU Shi-qing[1]

(1. *College of Materials Science and Engineering, China Jiliang University, Hangzhou* 310018, *China*;
2. *College of Materials and Environmental Engineering, Hangzhou Dianzi University, Hangzhou* 310018, *China*)

* *Corresponding Author, E-mail: dengdegang@cjlu.edu.cn*

Abstract: A two-peak adjustable semiconductor luminescent material $BaZn_2(BO_3)_2:xEu^{3+}$ phosphor was prepared by high temperature solid state method. The phosphor has a strong absorption in the ultraviolet band in the range of 300 to 400 nm. With the excitation of 375 nm, this phosphor exhibits two broad emission bands, peaked at 550 and 615 nm. And under the excitation of 393 nm, this phosphor exhibits a strong broad emission band, peaked at 615 nm due to the $^5D_0 \rightarrow {}^7F_2$ electric dipole transition of Eu^{3+}, which indicates that Eu^{3+} occupies an anti-inversion symmetry, and partly replaces the divalent Ba^{2+} in the $BaZn_2(BO_3)_2$ lattice. When the mole fraction of Eu^{3+} reaches 10%, the concentration quenching occurs. The color hue of $BaZn_2(BO_3)_2:xEu^{3+}$ phosphors under different doped concentrations of Eu^{3+} ions can be tuned from yellow to red.

Key words: phosphors; $BaZn_2(BO_3)_2:Eu^{3+}$; white LEDs
CLC number: O482.31 **Document code**: A **DOI**: 10.3788/fgxb20183904.0457

一种 LED 用红色荧光粉 $BaZn_2(BO_3)_2:Eu^{3+}$ 的合成与发光性能研究

吴程潇[1], 邓德刚[1*], 阮枫萍[1], 余 华[2], 徐时清[1]

(1. 中国计量大学 材料科学与工程学院, 浙江 杭州 310018;
2. 杭州电子科技大学 材料与环境工程学院, 浙江 杭州 310018)

摘要: 通过高温固相法制得双峰可调节本征半导体发光 $BaZn_2(BO_3)_2:Eu^{3+}$ 荧光粉,此类荧光粉在 300 ~ 400 nm 的紫外波段有很强的吸收。在 375 nm 的紫外光激发下,该荧光粉产生了两个宽带的发射峰,分别位于 550 nm 和 615 nm 处。并且,在 395 nm 的紫光激发下,荧光粉会由于 Eu^{3+} 离子的 $^5D_0 \rightarrow {}^7F_2$ 电偶极跃迁产生一个位于 615 nm 的强宽发射峰,这表明 Eu^{3+} 离子占据了反演对称中心的位置,取代了 $BaZn_2(BO_3)_2$ 中部分的 Ba^{2+} 离子。当 Eu^{3+} 的摩尔分数达到 10% 时,发生浓度猝灭。在不同浓度的 Eu^{3+} 离子的掺杂下,$BaZn_2(BO_3)_2:Eu^{3+}$ 荧光粉的发光从黄色延伸到红色,实现了荧光粉的色度可调。

关 键 词: 荧光粉; $BaZn_2(BO_3)_2:Eu^{3+}$; 白光 LED

收稿日期: 2017-08-15; **修订日期**: 2017-09-20
基金项目: 浙江省自然科学基金(LR14A040002, LQ13E020003, Y16F050012); 国家自然科学基金(61405185, 51272243, 61370049, 51402077, 61575182); 江苏省自然科学基金青年基金(BK20160905)资助项目
Supported by Zhejiang Provincial Natural Science Foundation of China(LR14A040002, LQ13E020003, Y16F050012); National Natural Science Foundation of China(61405185, 51272243, 61370049, 51402077, 61575182); Natural Science Youth Foundation of Jiangsu Province(BK20160905)

1 Introduction

WLED (White light-emitting diode) has broad application prospects because of the advantages such as low power consumption, long life and no pollution. At present, the research on luminescent materials, the society is still in the field of rare earth elements. The commercial white LED production is a combination of YAG: Ce^{3+} yellow phosphor and blue LED chip[1-3]. Part of the blue light emitted by the chip from the gaps in the phosphor powder, the rest of the phosphor converted to broadband emission of yellow light, and both of them are superimposed to get white light. However, the yellow light emitted by YAG: Ce^{3+} is lack of red light radiation, which leads to the low color rendering of white LED. There are two ways to solve the above problems: adding the red light phosphor emitted by blue light into the YAG: Ce^{3+} phosphor powder to improve the color rendering index of white light; exciting three primary phosphor by near ultraviolet or UV radiation InGaN chip to obtain high quantum efficiency white light[4]. In these two kinds of white LED, it is necessary to study the efficient red phosphors.

In recent years, rare earth ions have been widely studied as activators of fluorescent powder. Also, the Eu^{3+} ion is an ideal activator of red phosphor. The Eu^{3+} ion doped materials of LED has a very good absorption on the blue emission, but also a very high quantum efficiency under the excitation of UV light, especially Eu^{3+} ion occupys anti-inversion symmetry in the host, which has strong emission in red because of the $^5D_0 \rightarrow {}^7F_2$ transition[5-6].

For the advantages such as cheap raw materials, high stability and luminescence efficiency, optical properties of Eu^{3+} ion doped borate phosphor were widely studied over the past years[7-10]. The two-peak adjustable phosphor doped with a single rare earth Eu^{3+} ion in the host $BaZn_2(BO_3)_2$ has not yet been published. The 4f transition of Eu^{3+} ion is mainly due to the interaction of electric dipole and magnetic dipole[11-12]. The lattice symmetry is stronger, and the intensity of electric dipole transition is greater. However, the lattice symmetry has little effect on the magnetic dipole transition. Therefore, the Eu^{3+} ion is an ideal activator in lattice symmetry[13-15]. In this paper, the two-peak adjustable $BaZn_2(BO_3)_2:xEu^{3+}$ phosphor was prepared by high temperature solid state method, and then we studied the luminescent properties.

2 Experiments

The $BaZn_2(BO_3)_2:xEu^{3+}$ phosphors were prepared by high temperature solid state method, according to the chemical formula of weighing the materials $BaCO_3$ (A. R.), ZnO (99.99%), H_3BO_3 (A. R.) and Eu_2O_3 (99.99%), then thoroughly homogenized by grinding, and presintered in air at 850 ℃ for 4 h in muffle furnace. Then we reground the samples into powders.

A Bruker Axs D2 PHASER diffractometer with graphite monochromatized Cu Kα radiation (λ= 0.154 06 nm) was used to record the powder X-ray diffraction (XRD) data with 2θ ranging from 10° to 80°, operating at 10 mA and 30 kV. A PL3-211-P spectrometer (HORIBA JOBIN YVON, America) with a 450 W xenon lamp as the excitation source was employed to detect the excitation and emission spectra. The decay times were also measured using this equipment, and a pulsed spectral LED at 370 nm was excited, operating in the multichannel scaling mode. And we used the white powder $BaSO_4$ as a reference to text the diffuse reflectance spectra with a UV-3600 UV-Vis spectrometer (Shimadzu, Japan). The photoluminescence was measured by an exciting spectra and thermal quenching analyzer for phosphors (Everfine, China).

3 Results and Discussion

Fig. 1 (a) shows that the phosphor phase can be compared with the standard card in good agreement, which indicates the substitution of Eu^{3+} for Ba^{2+}, but no change of crystal structure. Also the peak position, with variation of concentration, the overall move to large angle direction, indicates that the small radius of Eu^{3+} ions replace the large radius of Ba^{2+} ions, which can be seen in Fig. 1(b).

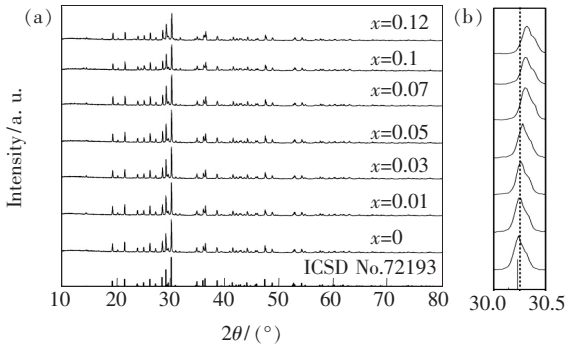

Fig. 1　(a) XRD patterns of $BaZn_2(BO_3)_2:xEu^{3+}$ ($x=0$, 0.01, 0.03, 0.05, 0.07, 0.1, 0.12) and the standard date card of ICSD-72193 as a reference; (b) Magnified XRD patterns in the region between 30.0° and 30.5°.

Fig. 2 show the refinement XRD patterns of $BaZn_2(BO_3)_2$ phosphor. The space group is $P2_12_12_1$, which are showed in Tab. 1. It is an orthorhombic cell with dimensions $a=0.932\ 7(7)$ nm, $b=1.211\ 9(6)$ nm, and $c=0.492\ 4(3)$ nm. Fig. 3 show the cell structure of $BaZn_2(BO_3)_2$. It exhibits a framework of that Ba atom is coordinated by six oxygen

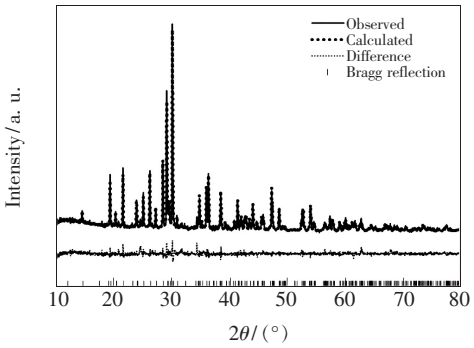

Fig. 2　Observed, calculated and difference synchrotron XRD profiles for the Rietveld refinement of $BaZn_2(BO_3)_2$. Bragg reflections are indicated with tick marks.

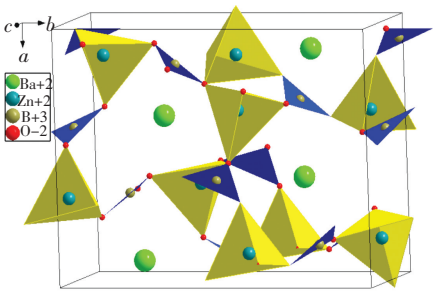

Fig. 3　Cell structure of $BaZn_2(BO_3)_2$ (black solid lines denote the unit cell)

atoms, BO_3 triangles and ZnO_4 tetrahedra that share vertices. There are two types of Zn atoms. A tetrahedral with the Zn atom as the center shares an O atom with the Ba atom, and the other shares two O atoms[12]. Final atomic coordinates and temperature factors for $BaZn_2(BO_3)_2$ host are shown in Tab. 2.

Tab. 1　Rietveld refinement and crystal data of $BaZn_2(BO_3)_2:0.1Eu^{3+}$ phosphors

Parameter	Occupancy
Formula	$BaZn_2(BO_3)_2:0.1Eu^{3+}$
Cryst. syst.	$P2_12_12_1(19)$-orthorhombic
Crystal density/(g · cm^{-3})	6.052
Units, Z	4
a/nm	0.932 696 93
b/nm	1.211 841 83
c/nm	0.492 413 69
V/nm^3	0.556 565 91
R_{exp}	7.23%
R_{wp}	11.55%
R_p	8.28%
GOF	1.60

Tab. 2　Final atomic coordinates and temperature factors for $BaZn_2(BO_3)_2$ host

Atom	x	y	z	Occupancy
Ba1	0.396 49	0.229 91	0.031 59	0.952 3
Zn1	0.370 08	0.895 38	0.039 60	1.256
Zn2	0.657 59	0.031 04	0.944 33	1.071
B1	0.438 89	−0.069 96	0.427 36	2.547
B2	0.600 38	0.215 14	0.535 25	4.485
O1	0.584 01	0.269 36	0.644 72	0.278 7
O2	0.327 49	0.077 20	0.438 46	1.455
O3	0.230 91	0.422 68	0.355 00	1.097
O4	0.487 03	−0.003 87	0.819 56	1.97
O5	0.614 25	0.329 80	−0.085 77	1.669
O6	0.680 27	0.152 96	0.237 67	2.79

There is a strong reflection from 400 to 800 nm in host $BaZn_2(BO_3)_2$ and an obvious absorption at the range of 200 – 400 nm because of the energy transition between conduction and valence band, which can be seen clearly in Fig. 4(a). As $BaZn_2(BO_3)_2:xEu^{3+}$ shows that a narrowband absorption near 465 nm at the band, which is due to the

absorption of Eu^{3+} on the $^7F_0 \rightarrow {}^5D_2$ transition. In fact, there should be a Eu^{3+} on the $^7F_0 \rightarrow {}^5L_6$ transition absorption in the vicinity of 396 nm, but for the strong host absorption in the ultraviolet band, the absorption of Eu^{3+} is not obvious. The absorption spectrum of Eu^{3+} ions is caused by the internal f-f transition, which is influenced by the external electrons. But the host of the crystal field has a small effect on the absorption. The absorption spectra of Eu^{3+} in $BaZn_2(BO_3)_2$: xEu^{3+} samples are the same shape as those of the narrow band absorption spectra of the f-f transition, and the absorption peak position does not appear a obvious shift. According to the spectrum[16-17], the electric dipole transition $L=0$ is forbidden, but due to the deviation of the inversion center and the configuration of 4f, the parity opposite configuration G or configuration D mixed, such f-f transitions become allowed.

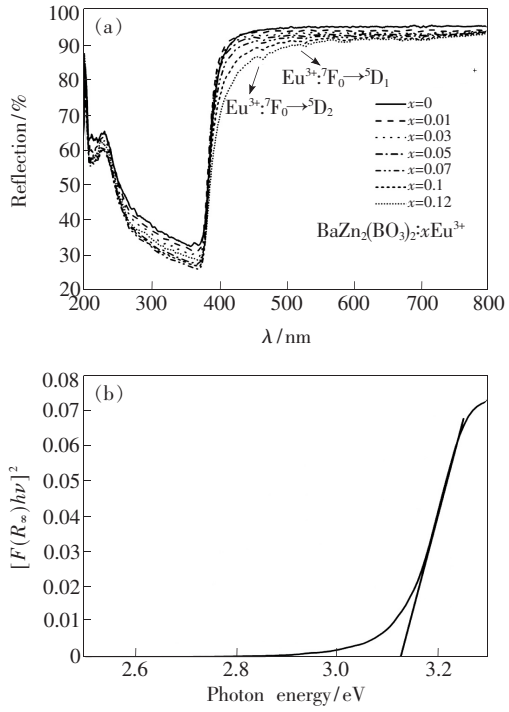

Fig. 4 (a) Diffuse reflection spectra of $BaZn_2(BO_3)_2$: xEu^{3+} (x = 0, 0.01, 0.03, 0.05, 0.07, 0.1, 0.12). (b) Absorption spectra of $BaZn_2(BO_3)_2$ as calculated by the Kubelka-Munk formula.

The band-gap of $BaZn_2(BO_3)_2$ host can be calculated according to formula (1)[18]:

$$[F(R_\infty)h\nu]^n = A(h\nu - E_g), \qquad (1)$$

where $F(R_\infty)$ is the Kubelka-Munk function, $n=2$ for an direct transition or 1/2 for an indirect transition, $h\nu$ represents the photon energy, A is constant, and E_g is the value of the band gap. $BaZn_2(BO_3)_2$ is a direct band-gap semiconductor, so the value of n is 2. The absorption spectra of $BaZn_2(BO_3)_2$ host can be got from the diffuse reflection by using the Kubelka-Munk function[19]:

$$F(R_\infty) = (1-R)^2/2R = K/S, \qquad (2)$$

where R is the reflectance, K and S are the absorption and the scattering coefficients, respectively. Fig. 4(b) presents the absorption spectra of $BaZn_2(BO_3)_2$ derived with the Kubelka-Munk function. For $BaZn_2(BO_3)_2$ from the linear extrapolation of

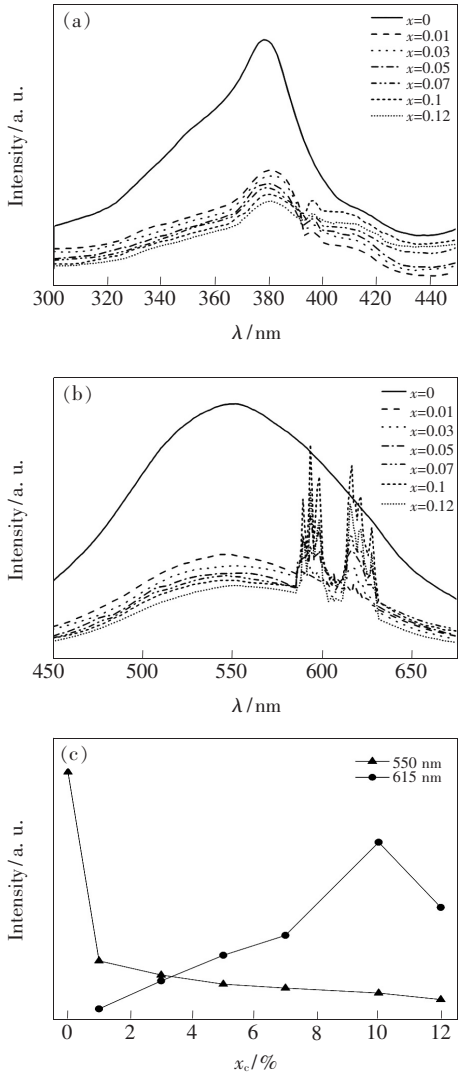

Fig. 5 (a) Photoluminescence excitation spectra of $BaZn_2(BO_3)_2$: xEu^{3+} phosphors. (b) Photoluminescence spectra of $BaZn_2(BO_3)_2$: xEu^{3+} phosphors under the excitation of 375 nm. (c) The change trend of emission intensity of two peaks.

$K/S=0$, E_g value was calculated to be about 3.12 eV. According to the band-gap width of semiconductors, they are divided into narrow band-gap semiconductor ($E_g<2$ eV), wide band-gap semiconductor ($E_g>2$ eV) and gapless semiconductor ($E_g\sim0$ eV). It is obvious that $BaZn_2(BO_3)_2$ belongs to wide band-gap semiconductor like ZnO (3.37 eV) and SiC (2.2 eV).

As it shown in Fig. 5(a), when the emission peak 550 nm is used to monitor the excitation spectrum, there is a strong excitation peak at 375 nm in the host. And with the Eu^{3+} ion concentration increasing, the excitation peak appears at 393 nm, which is due to the $^7F_0\rightarrow{}^5L_6$(393 nm) transition of Eu^{3+} ion. However, when the mole fraction of Eu^{3+} is 10%, the intensity of the peak begins to decline due to the concentration quenching. In Fig. 5(b), we find that when we increase the doped concentration of Eu^{3+} ions, the emission of host at the 550 nm is gradually weakened, and the emission spectrum in the vicinity of 615 nm belongs to the Eu^{3+} ions $^5D_0\rightarrow{}^7F_1$ or $^7F_2$ significantly enhanced, which further shows that the energy transfer from the host to the Eu^{3+} promotes the luminescence of Eu^{3+} in the host. When the mole fraction of Eu^{3+} reaches 10%, the concentration quenching occurs, which are shown in Fig. 5(c).

The excitation spectra of the $BaZn_2(BO_3)_2:xEu^{3+}$ samples are recorded between 350 and 450 nm by monitoring the $^5D_0\rightarrow{}^7F_2$ emission at 615 nm. It can be seen from Fig. 6(a), The sharp intense excitation peaks of Eu^{3+} ions from 300 to 450 nm include $^7F_0\rightarrow{}^5L_7$ (385 nm), $^7F_0\rightarrow{}^5L_6$ (392 – 400 nm), and $^7F_0\rightarrow{}^5D_3$(415 nm) emissions[10,20]. And the strong excitation at 393 nm is used to monitor the excitation for emission spectra of the phosphor. The wavelength band of Eu^{3+} is relatively narrow, and the wavelength is mainly located in the orange and red range. Eu^{3+} emission spectrum is the energy of the electron from the state $^5D_0$ to state ^7F_J($J=0$, 1, 2, 3, 4). When Eu^{3+} is in a different lattice position, the intensity of the transition is different. When the $^5D_0\rightarrow{}^7F_1$ radiative transition occurs, Eu^{3+} is the center of inversion in the lattice; when the $^5D_0\rightarrow{}^7F_2$ and $^5D_0\rightarrow{}^7F_4$ radiative transitions occur, Eu^{3+} is the center of non inversion in the lattice. There are many strong emission peaks in the emission spectra of 500 – 700 nm, and the emission peaks in this range are composed of the $^5D_0\rightarrow{}^7F_J$ ($J=0$, 1, 2, 3, 4) energy transition of Eu^{3+}. The characteristic emission peaks of five Eu^{3+} ions are shown in Fig. 6(b): the emission of $^5D_0\rightarrow{}^7F_0$ and $^5D_0\rightarrow{}^7F_3$ corresponding to the emission bands near 580 nm and 653 nm is smaller, while the emission peaks in the corresponding emission band 590 nm, near 615 nm and 683 nm appeared in $^5D_0\rightarrow{}^7F_1$, $^5D_0\rightarrow{}^7F_2$ and $^5D_0\rightarrow{}^7F_4$ transition are obvious. The 590 nm transition is the magnetic dipole transition in the five transition bands,

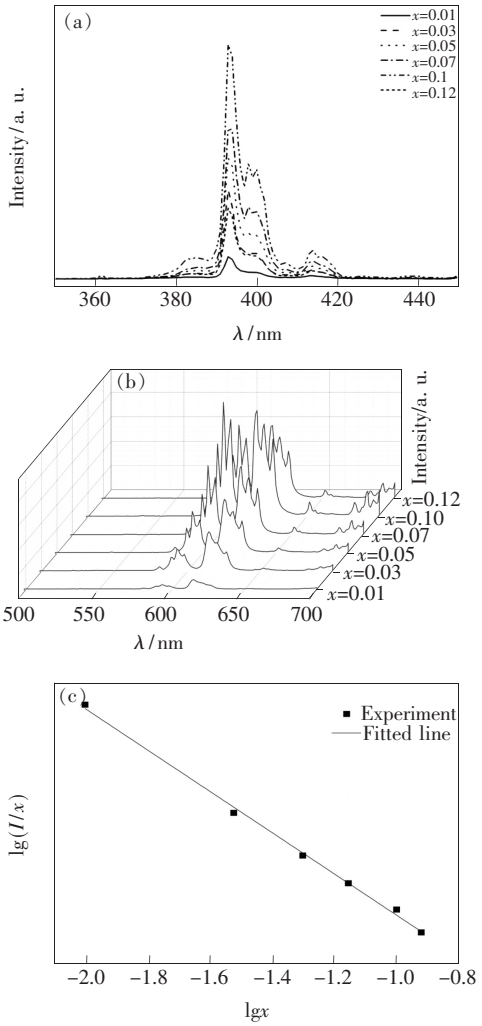

Fig. 6　(a) Photoluminescence excitation spectra of $BaZn_2(BO_3)_2:xEu^{3+}$ phosphors. (b) Photoluminescence spectra of $BaZn_2(BO_3)_2:xEu^{3+}$ phosphors under the excitation of 393 nm. (c) Relationship between lg$x$ and lg(I/x).

and the $^5D_0 \rightarrow {}^7F_2$ transition in the vicinity of 615 nm is an electric dipole transition. The intensity ratio of the characteristic diffraction peaks produced by $^5D_0 \rightarrow {}^7F_2$ and $^5D_0 \rightarrow {}^7F_1$ transitions can be used to determine the coordination environment of Eu^{3+} ions. The $^5D_0 \rightarrow {}^7F_2$ electric dipole transition occurs and the red light (about 615 nm) is dominated by $^5D_0 \rightarrow {}^7F_2$ electric dipole transition[21]. It can be seen from the figure, at the beginning, the emission intensity of $^5D_0 \rightarrow {}^7F_2$ was significantly higher than that of other emission peaks, but with the increase of ion concentration in $BaZn_2(BO_3)_2:xEu^{3+}$, the two peaks began to increase and sharpening, and split, and the asymmetry ratio is smaller than the orange (R/O). It is found that $BaZn_2(BO_3)_2:Eu^{3+}$ phosphor is a kind of potential red phosphor for white LED with excitation and emission spectra.

With the formula given by Blasse and Grabmaier[22], we have calculated the value of critical distance between the Eu^{3+} ions:

$$R_c \approx 2[3V/4\pi x_c Z]^{1/3}, \quad (3)$$

where V is the unit cell volume, x_c and Z are the quenching concentration of activator and the value of formula units per unit cell. For $BaZn_2(BO_3)_2$ host, using $Z=4$, $x_c=0.1$ and $V=0.556\ 565\ 91\ nm^3$, then the obtained R_c is 0.673 nm.

From Dexter's theory, we get the energy transfer between Eu^{3+} ions is due to the electric multipole-multipole interactions[23]. When it occurs among the same types of activators, the extent of the interactions can be revealed from the change intensity of emission. The emission intensity per activator ion can be calculated by the formula[24-25]:

$$I/x = k[1+\beta(x)^{Q/3}]^{-1}, \quad (4)$$

where I represents the intensity of emission, x is the concentration of activator, k and β are constants; while $Q=3$, 6 or 8 is for the energy transfer between the nearest-neighbor, dipole-dipole or dipole-quadrupole ions respectively, and $Q=10$ is for the quadrupole-quadrupole interactions. Fig. 6(c) shows that the relationship between $\lg(I/x)$ and $\lg x$ is linear and the value of slope is -0.74. From the above formula (4), the value of Q was calculated to be 2.32, which is closed to 3. It indicates that the main mechanism of concentration quenching of the Eu^{3+} emission in $BaZn_2(BO_3)_2:xEu^{3+}$ phosphors is the energy transfer among the nearest neighbor ions.

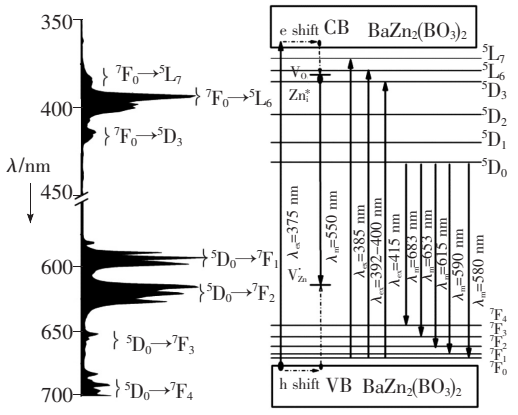

Fig. 7 Energy level diagram of the $BaZn_2(BO_3)_2$ host, Eu^{3+} and schematic of the energy transfer mechanism from the $BaZn_2(BO_3)_2$ host to Eu^{3+}.

Under the UV excitation at 375 nm, electrons in host $BaZn_2(BO_3)_2$ are excited from the valence band to conduction band. The photogenerated holes in the valence band are trapped by a single negatively charged oxygen interstitial ion center O_i^- and combined with the photogenerated electrons falling off the conduction band to produce photons through non-radiative processes[26]. The electrons can also transfer their energy to the $^5D_0$ level of Eu^{3+}. The radiative transition of Eu^{3+}: $^5D_0 \rightarrow {}^7F_J$ ($J=0$, 1, 2, 3, 4) results in yellow pink to reddish orange PL. This is schematically shown in Fig. 7.

Fig. 8(a) and (b) illustrate the fluorescence decay curves of $BaZn_2(BO_3)_2$ and $BaZn_2(BO_3)_2:xEu^{3+}$ phosphors at room temperature monitored at 550 nm, the $BaZn_2(BO_3)_2:xEu^{3+}$ phosphors monitored at 615 nm respectively. In general way, with the concentration of activators increasing, the distance between them decreases and thus energy transfer among them occurs. With various concentrations of activators, the decay times are different[27-30]. There are two luminescence centers in $BaZn_2(BO_3)_2:xEu^{3+}$, so that we can fit the decay curves with the double-exponential equation[31]:

$$I(t) = A_1\exp(-t/\tau_1) + A_2\exp(-t/\tau_2), \quad (5)$$

where $I(t)$ represents the intensity of emission at

time t, A_1 and A_2 are constants, t is time, τ_1 and τ_2 are the exponential components of decay times. The following equation can be used to calculate the average decay times (τ)[32]:

$$\tau = (A_1\tau_1^2 + A_2\tau_2^2)/(A_1\tau_1 + A_2\tau_2), \quad (6)$$

when monitored at 550 nm, the lifetime of the $BaZn_2(BO_3)_2$ host is calculated to be 0.15 ms. There are no obvious difference among the lifetimes of $BaZn_2(BO_3)_2:xEu^{3+}$ ($0.01 \leqslant x \leqslant 0.12$) phosphors. We calculate the average value of their lifetimes is about 0.14 ms. While monitored at 615 nm, the lifetimes of $BaZn_2(BO_3)_2:xEu^{3+}$ ($0.01 \leqslant x \leqslant 0.12$) are determined from 1.20 ms to 2.20 ms. With the doping of Eu^{3+}, the lifetime of 550 nm becomes shorter, furthermore the lifetime of 615 nm increases gradually with the increasing doped concentrations of Eu^{3+}. It indicates that the energy transfer occurs from $BaZn_2(BO_3)_2$ host to Eu^{3+} ions.

Fig. 9 shows the CIE chromaticity coordinates for the $BaZn_2(BO_3)_2:xEu^{3+}$ phosphors with different x values. The color hue can be tuned from yellow to red, and the corresponding chromaticity coordinates (x, y) varying from (0.458 0, 0.338 7) to (0.616 7, 0.346 1) summarized in the inset table. It indicates the $BaZn_2(BO_3)_2:xEu^{3+}$ phosphors would be a potential color coordinate adjustable phosphor for using in white light-emitting diode.

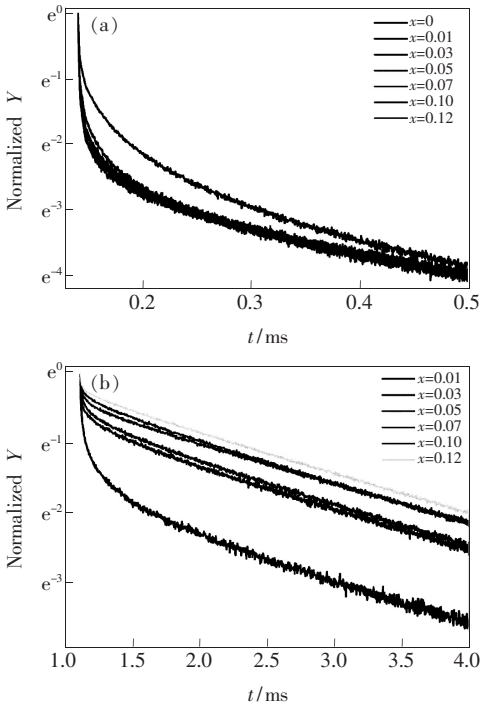

Fig. 8　(a) Decay profiles of $BaZn_2(BO_3)_2:xEu^{3+}$ phosphor monitored at 550 nm. (b) Decay profiles of $BaZn_2(BO_3)_2:xEu^{3+}$ phosphor at 615 nm.

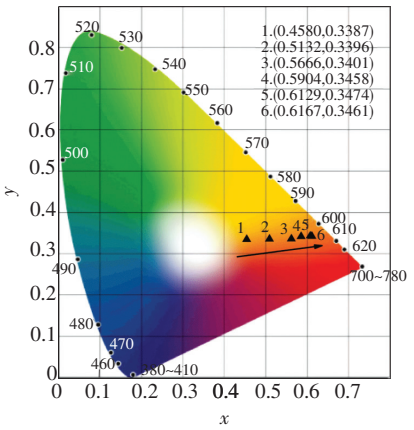

Fig. 9　CIE chromaticity diagram of $BaZn_2(BO_3)_2:xEu^{3+}$ phosphors excited at 393 nm (x = 0.01, 0.03, 0.05, 0.07, 0.1, 0.12), the inset shows the phosphors together with their photos taken under 393 nm excitation.

4　Conclusion

$BaZn_2(BO_3)_2:xEu^{3+}$ phosphor was prepared by high temperature solid state method. The excitation peak position of the host is located at 375 nm, the excitation peak of Eu^{3+} is located at 392 nm, and the peak of the emission spectrum is located near 550 nm and 615 nm. The emission of wavelengths at 550 nm is due to the semiconductor luminescence of the host itself, and emission at 615 nm is due to the $^5D_0 \rightarrow {}^7F_2$ transition of Eu^{3+}. And with the addition of Eu^{3+} ions, the energy of the host transfers to the Eu^{3+}. When the doping concentration is 10%, $BaZn_2(BO_3)_2:0.1Eu^{3+}$ phosphor with excellent performance in various aspects has a strong red emission from580 to 630 nm, and also a potential application in white LED.

References:

[1] YAO G Q, DUAN J F, REN M, *et al.*. Preparation and luminescence of blue light conversion material YAG:Ce [J]. *J. Lumin.*, 2001, 22:22-26.

[2] XU Y, CHEN L H, LI Y Z. Phosphor-conversion white light using InGaN ultraviolet laser diode [J]. *Appl. Phys. Lett.*, 2008, 92:021129.

[3] LIN C C, LIU R S. Advances in phosphors for light-emitting diodes [J]. *Phys. Chem. Lett.*, 2011, 2:1268.

[4] YAN B, LIN L, WU J, *et al.*. Photoluminescence of rare earth phosphors $Na_{0.5}Gd_{0.5}WO_4:RE^{3+}$ and $Na_{0.5}Gd_{0.5}(Mo_{0.75}W_{0.25})O_4:RE^{3+}$ (*RE* = Eu, Sm, Dy) [J]. *J. Fluoresc.*, 2011, 21:203-211.

[5] ZENG X Q, SEOUNG-JAE I M, JANG S H, *et al.*. Luminescent properties of $(Y, Gd)BO_3:Bi^{3+}$, RE^{3+} (*RE* = Eu, Tb) phosphor under VUV/UV excitation [J]. *J. Lumin.*, 2006, 121(1):126.

[6] TIAN L H, KIM S J, PARK H L, *et al.*. Variation of the photoluminescence and vacuum ultraviolet excitation characteristics of $BaZr(BO_3)_2:Eu^{3+}$ by the incorporation of Al^{3+}, La^{3+}, or Y^{3+} into the lattice [J]. *Mater. Res. Bull.*, 2006, 41(1):29-37.

[7] SUN L D, QIAN C, LIAO C S, *et al.*. Luminescence phosphors of Li^+ doped nanosized $Y_2O_3:Eu^{3+}$ [J]. *Solid State Commun.*, 2001, 119(6):393-396.

[8] WANG Z L, LIANG H B, GONG M L, *et al.*. Luminescence investigation of Eu^{3+} activated double molybdates red phosphors with scheelite structure [J]. *J. Alloys Compd.*, 2007, 432:308-312.

[9] FENG G, JIANG W H, CHEN Y B, *et al.*. A novel red phosphor $NaLa_4(SiO_4)_3F:Eu^{3+}$ [J]. *Mater. Lett.*, 2011, 65(1):110-112.

[10] DENG D G, YU H, HUA Y J, *et al.*. $Ca_4(PO_4)_2O:Eu^{2+}$ red-emitting phosphor for solid-state lighting: structure, luminescent properties and white light emitting diode application [J]. *J. Mater. Chem.* C, 2013, 1:3194-3199.

[11] CHEN C, WU B, JIANG A, *et al.*. A new-type ultraviolet SHG crystal—β-BaB_2O_4 [J]. *China Ser.* B, 1985, 28: 235-243.

[12] SMITH R W, KESZLER D A. The noncentrosymmetric orthoborate $BaZn_2(BO_3)_2$ [J]. *Solid State Chem.*, 1992, 100: 325-330.

[13] CHEN F, YUAN X, ZHANG F, *et al.*. Photoluminescence properties of $Sr_3(PO_4)_2:Eu^{2+}$, Dy^{3+} double-emitting blue phosphor for white LEDs [J]. *Opt. Mater.*, 2014, 37:65-69.

[14] DORENBOS P. Energy of the first $4f^7 \rightarrow 4f^6 5d$ transition of Eu^{2+} in inorganic compounds [J]. *J. Lumin.*, 2003, 104: 239-260.

[15] XIE R J, HIROSAKI N, MITOMO M, *at al.*. Optical properties of Eu^{2+} in-SiAlON [J]. *Phys. Chem.* B, 2004, 108:12027.

[16] HARANATH D, SHANKER V, CHANDER H, *et al.*. Tuning of emission colours in strontium aluminate long persisting phosphor [J]. *J. Appl. Phys.*, 2003, 36:2244-2248.

[17] JIE L, LIAN H Z, SHI C S. Improved optical photoluminescence by charge compensation in the phosphor system $CaMoO_4:Eu^{3+}$ [J]. *Opt. Mater.*, 2007, 29(12):1591-1594.

[18] CHEN F, YUAN X, ZHANG F, *et al.*. Photoluminescence properties of $Sr_3(PO_4)_2:Eu^{2+}$, Dy^{3+} double-emitting blue phosphor for white LEDs [J]. *Opt. Mater.*, 2014, 37:65-69.

[19] WANG Z, LIANG H, GONG M, *et al.*. Luminescence investigation of Eu^{3+} activated double molybdates red phosphors with scheelite structure [J]. *J. Alloys Compd.*, 2007, 432(1-2):308-312.

[20] CHEN X Y, LIU G K. The standard and anomalous crystal-field spectra of Eu^{3+} [J]. *Solid State Chem.*, 2005, 178:419-428.

[21] GUO N, HUANG Y J, YOU H P, *et al.*. $Ca_9Lu(PO_4)_7:Eu^{3+}$, Mn^{2+}: a potential single-phased white-light-emitting phosphor suitable for white-light-emitting diodes [J]. *Inorg. Chem.*, 2010, 49(23):10907-10913

[22] BLASSE G. Energy transfer in oxidic phosphors [J]. *Philips Res. Rep.*, 1969, 24:131-144.

[23] YU H, DENG D G, LI Y Q, *et al.*. Luminescent properties of red-emitting $LiSr_4B_3O_{(9-3x/2)}N_x:Eu^{2+}$ phosphor for white-LEDs [J]. *Opt. Commun.*, 2013, 289:103-108.

[24] LIU H, ZHANG Y, LIA L, *et al.*. Synthesis, broad-band absorption and luminescence properties of blue-emitting phosphor $Sr_8La_2(PO_4)_6O_2:Eu^{2+}$ for n-UV white-light-emitting diodes [J]. *Ceram. Int.*, 2014, 40:13709-13713.

[25] LI K, GENG D, SHANG M, *et al.*. Color-tunable luminescence and energy transfer properties of $Ca_9Mg(PO_4)_6F_2:Eu^{2+}$, Mn^{2+} phosphors for UV-LEDs [J]. *J. Phys. Chem.* C, 2014, 118:11026-11034.

[26] WANG Z L, LIN C K, LIU X M, *et al.*. Tunable photoluminescent and cathodoluminescent properties of ZnO and ZnO: Zn phosphors [J]. *J. Lin. Phys. Chem.* B, 2006, 110:9469-9476.

[27] LI H, ZHAO R, JIA Y, *et al.*. $Sr_{1.7}Zn_{0.3}CeO_4:Eu^{3+}$ novel red-emitting phosphors: synthesis and photoluminescence

properties [J]. *ACS Appl. Mater. Interf.*, 2014, 6:3163-3169.

[28] SOHN K S, CHOI Y Y, PARK H D. Photoluminescence behavior of Tb^{3+}-activated YBO_3 phosphors [J]. *J. Electrochem. Soc.*, 2000, 147:1988-1992.

[29] HUANG C H, KUO T W, CHEN T M. Novel red-emitting phosphor $Ca_9Y(PO_4)_7:Ce^{3+}$, Mn^{2+} with energy transfer for fluorescent lamp application [J]. *ACS Appl. Mater. Interf.*, 2010, 2:1395-1399.

[30] LV W, JIA Y, ZHAO Q, *et al.*. Synthesis. structure. and luminescence properties of $K_2Ba_7Si_{16}O_{40}:Eu^{2+}$ for white light emitting diodes [J]. *J. Phys. Chem.* C, 2014, 118:4649-4655.

[31] YU H, DENG D G, XU S Q, *et al.*. Luminescent properties of novel $Ca_{2.89}Mg_{0.11}(PO_4)_2:Eu^{2+}$ single-phase white light-emitting phosphor for white LEDs [J]. *Ceram. Int.*, 2015, 41:3800-3805.

[32] DEXTER D, SCHULMAN J H. Theory of concentration quenching in inorganic phosphors [J]. *J. Chem. Phys.*, 1954, 22:1063-1070.

吴程潇(1992 –),男,安徽太湖人,硕士研究生,2015 年于安徽科技学院获得学士学位,主要从事稀土发光方面的研究。

E-mail: 18867141292@163.com

邓德刚(1975 –),男,湖北仙桃人,博士,教授,硕士生导师,2007 年于中科院上海光机所获得博士学位,浙江省 151 第二层次资助人员,主要从事稀土掺杂玻璃和光纤、半导体照明用发光材料、特种玻璃等光电功能材料及器件的研究。

E-mail: dengdegang@cjlu.edu.cn